LBl-17267 c.2
Preprint

Lawrence Berkeley Laboratory

UNIVERSITY OF CALIFORNIA

Materials & Molecular Research Division

RECEIVED
LAWRENCE
BERKELEY LABORATORY
MAR 14 1984
LIBRARY AND
DOCUMENTS SECTION

Submitted to Applied Physics Letters

HIGH RESOLUTION TRANSMISSION ELECTRON MICROSCOPY STUDY OF Se^+ IMPLANTED AND ANNEALED GaAs: MECHANISMS OF AMORPHIZATION AND RECRYSTALLIZATION

D.K. Sadana, T. Sands, and J. Washburn

December 1983

TWO-WEEK LOAN COPY

This is a Library Circulating Copy which may be borrowed for two weeks. For a personal retention copy, call Tech. Info. Division, Ext. 6782.

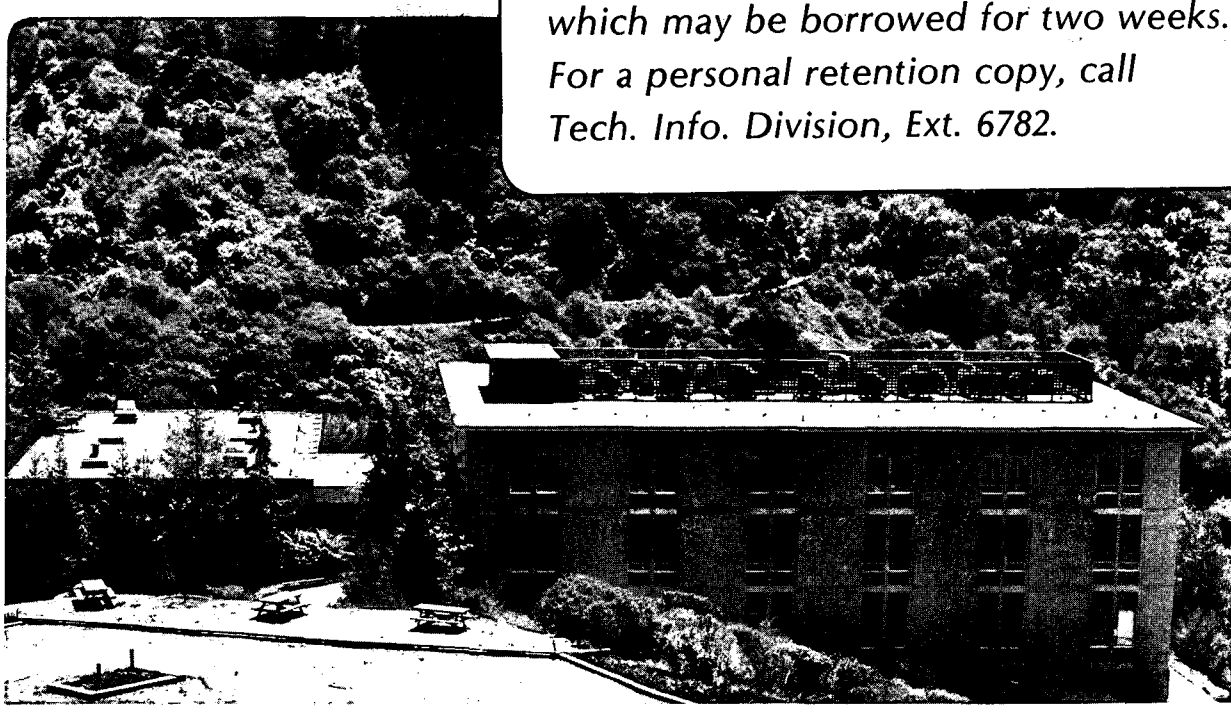

LBL-17267 c.2

Prepared for the U.S. Department of Energy under Contract DE-AC03-76SF00098

DISCLAIMER

This document was prepared as an account of work sponsored by the United States Government. While this document is believed to contain correct information, neither the United States Government nor any agency thereof, nor the Regents of the University of California, nor any of their employees, makes any warranty, express or implied, or assumes any legal responsibility for the accuracy, completeness, or usefulness of any information, apparatus, product, or process disclosed, or represents that its use would not infringe privately owned rights. Reference herein to any specific commercial product, process, or service by its trade name, trademark, manufacturer, or otherwise, does not necessarily constitute or imply its endorsement, recommendation, or favoring by the United States Government or any agency thereof, or the Regents of the University of California. The views and opinions of authors expressed herein do not necessarily state or reflect those of the United States Government or any agency thereof or the Regents of the University of California.

HIGH RESOLUTION TRANSMISSION ELECTRON MICROSCOPY STUDY OF Se^+ IMPLANTED AND ANNEALED GaAs: MECHANISMS OF AMORPHIZATION AND RECRYSTALLIZATION

D.K. Sadana*, T. Sands and J. Washburn
Materials and Molecular Research Divisions
Lawrence Berkeley Laboratory
University of California
Berkeley, California 94720

ABSTRACT

High resolution transmission electron microscopy (HRTEM) has been applied to the study of amorphization and recrystallization mechanisms in Se^+ implanted (100) GaAs. Selenium dose of 1 x 10^{14} cm^{-2} at 450 keV (projected range 1550Å) produced an amorphous band in the depth range 250 to 2150Å below the surface. Annealing at 400°C resulted in the epitaxial regrowth of the upper and lower transition region (0-250Å and 2150-2500Å, respectively). Regrowth of the amorphous layer was found to proceed by the nucleation and propagation of the dense network of stacking fault bundles. Amorphization and recrystallization mechanisms in Se^+ implanted GaAs are discussed in light of these HRTEM results.

*Now at Microelectronics Center of North Carolina
Research Triangle Park, North Carolina 27709

Conventional (bright-field and weak-beam) transmission electron microscopy (TEM) and Rutherford backscattering (RBS) / channeling have been utilized extensively for structural examination of ion implanted and subsequently annealed GaAs.[1-7] It is known from these measurements that amorphous layers produced by ion implantation recrystallize at a much lower temperature (150-200°C)[1-7] than analogous amorphous layers of Si (450°C). Another important difference in the recrystallization behavior of these two materials is that regrowth of amorphous layers in (100) Si can result in essentially defect-free material, whereas regrowth of amorphous GaAs layers in (100) GaAs usually results in microtwins, stacking faults, misoriented crystallites and other irregular structures [1,4,6,7]. These differences are also reflected in the electrical behavior of recrystallized layers. For example, the optimum electrical activation (90-100%) of dopants in Si is achieved when the implanted region is completely amorphized before annealing. However, in GaAs such conditions result in the lowest activation of dopants (~10%).[4,8] Better electrical results in GaAs have been reported for elevated temperature (>100°C) implants for which amorphization of the implanted region does not occur.[9] It is therefore apparent that more detailed characterization of amorphized and regrown GaAs is necessary. In this communication, the high resolution TEM (HRTEM) and conventional TEM results from Se implanted and furnace annealed GaAs are presented along with a phenomological discussion of GaAs amorphization and recrystallization mechanisms.

Selenium ions accelerated to 450 keV were implanted at nominal room temperature into semi-insulating Cr-doped (100) GaAs samples to a dose of 10^{14} cm^{-2}. The implanted samples were capped with Al and then annealed in a furnace in the temperature range 400-800°C. For TEM analysis, specimens of both plan and cross-sectional geometries were used. The former were prepared by chemical (methanol + 3% Cl_2) thinning from the unimplanted side. The latter were prepared by Ar^+ ion milling at LN_2 temperature (4.5kV, 20μ A specimen current, 14° tilt). Room temperature ion milling caused in situ annealing of the amorphous layer. A JEOL 200 CX HRTEM (Cs≃1.2 mm, top entry stage) was used to obtain HRTEM images in <011> zone axis orientation from cross-section specimens.

Figure 1 is a set of cross-sectional TEM micrographs from the unannealed (Fig. 1a) and 400°C annealed (Fig. 1b) samples. The unannealed sample contained three distinguishable damage regions: (I) an amorphous layer between 250 and 2150Å below the surface, (II) two heavily damaged amorphous/crystalline transition regions in the depth ranges 0-250Å and 2150-2500Å and (III) a lightly damaged crystalline region in the depth range 2500-3000Å.

The micrograph of the annealed sample shows that region I of the unannealed sample was converted into a dense crystalline band of microtwins and fault bundles (on {111}) which grew from both sides of the amorphous region and met at a depth of 1100Å. The

inset diffraction pattern (Fig. 1b) also shows spots from the $[\bar{2}110]$ zone of wurtzite, suggesting that some of the faults were bundled in such a sequence as to produce thin plates of wurtzite (e.g., an extrinsic fault adjacent to an intrinsic fault is equivalent to 4 layers of wurtzite: AaBb/Aa/CcAa/CcAaBb). The damage in regions II, III and beyond converted into small dislocation loops on annealing. The density of the loops decreased with depth.

HRTEM of regions I, II and III was performed using an objective aperture that contained all beams visible in the diffraction pattern (inset) of Fig. 1a or 1b. The following refinements to the results obtained by conventional TEM were made:

i) Region I was found to be completely amorphous (except near the boundary with regions II).

ii) The heavily damaged material in regions II of the unannealed sample was found to consist of an intimate mixture of small (500-150Å in diameter) amorphous and crystalline pockets. Many microtwin nuclei and small (~50Å) stacking faults were present in the regions II. These nuclei were found at amorphous-crystalline interfaces which were micro-faceted on {111}.[10]

iii) Rod-shaped defects approximately 30Å long and lying along <110> directions were found in the regions II and III in the unannealed sample. Figure 2 shows several of these defects near the boundary between regions II and III. The density of these defects in region III was estimated to be 5×10^{11} cm^{-2} (±50%), which is numerically equal to 0.5% of the total Se^+ dose. We propose that these defects are damage cascades to either channeling of Se^+ ions at the end of their tracks or channeling of recoiled Ga or As.

iv) HRTEM of the annealed sample showed that region II had recrystallized epitaxially but was not defect-free. Both perfect dislocations and isolated small stacking faults (projected length 50-150Å) bounded by Shockley partials were found in this region [see Fig. 3].

v) HRTEM of the annealed sample also confirmed that region I had completely recrystallized in the form of fault bundles and microtwins up to 10 atomic layers (~33Å) thick. These faults and twins nucleated at both top (~250Å) and bottom (~2150Å) interfaces and grew until impingement at a depth of 1100Å. Figure 4 is an HRTEM image of a fault bundle, suspected to be one of the first to nucleate since it extended all of the way to the impingement zone at 1100Å.

vi) After annealing, no evidence of channeled cascades was found. Instead, small (~35Å in diameter) extrinsic Frank dislocation loops (b || <111>) were found in the depth regions 3000 to 3500Å.

Based upon the HRTEM results discussed above, we propose the following model for the amorphization and recrystallization of GaAs. During the early stages of implantation, while the GaAs is still crystalline, either a small fraction of Se^+ ions (probably 0.5%) or a fraction of the recoiled Ga and As are channeled into <110> directions resulting in the cylindrical damage zones observed in region III (Fig. 2). That channeling is the major reason for these zones is supported by the observation on similar defects in (110) GaAs implanted with light ions such as oxygen.

The distinct two-phase nature of the transition region II[10] suggests that the amorphous state is formed by relaxation of crystalline material when the defect density reaches some critical value and that there is a competition between formation of amorphous zones and their epitaxial regrowth by dynamic annealing process. A similar model for the crystalline to amorphous transformation has been proposed for silicon.[11]

Dynamic annealing during the nominal room temperature implant results in the formation of microfacets on the crystalline pockets in the transition region II. In addition, dynamic regrowth of the crystalline pockets during implantation leads to the formation of stacking fault nuclei.[10]

Recrystallization during the 400°C annealing treatment occurs in two stages. THe first stage involves the complete epitaxial regrowth of the transition region. The fault nuclei present in the unannealed sample grow until they reach the growth front of a neighboring crystallites. Formation of stacking fault bundles or twins is impossible in this region due to the large number of growth fronts in various orientations. The rough nature of the boundary between regions I and II and the fact that <111> is the slowest growing direction eventually results in a microfaceted and simply connected growth front at a depth of approximately 2150Å (a similar process is occuring near the upper surface). Stage two in the regrowth process begins at this microfaceted growth front (facets on {111} have dimensions on the order of 50 to 100Å as judged from the size of the stacking fault bundles (see Fig. 4)).

The {111} facets provide favorable sites for accomodation of dopant concentration above the solid solubility limit and non-stoichiometry which was produced by the implantation and accumulated during the last part of stage one. Schockley partial dislocation cores form on the defected facets, thereby forming the nuclei for stacking fault bundles. Once a bundle of stacking faults has been nucleated, the propogation of the bundle is likely to be rapid because excess Ga or As and dopant atoms can be efficiently rejected to the amorphous material. Stage II is complete when stacking fault bundles from both interfaces meet in the middle of region I. Excess point defects and non-

stoichiometry in region III and below is accommodated by the formation of the small extrinsic Frank loops.

Finally, microtwin growth due to stacking errors is also encountered in the regrowth of amorphized (111) Si. However, such morphologies are not generally found in recrystallized (100) silicon. It is likely that many observed differences between the behavior of (100) GaAs and (100) Si are a result of the binary nature of GaAs. For example, the different displacement properties of Ga and As result in deviations in local stoichiometry which cannot be fully eliminated by low temperature annealing. These deviations in stoichiometry, along with impurities present above the solid solubility, are probably accommodated by extrinsic Frank loops, Shockley partial cores, perfect dislocation cores and defects at regrowth front intersections.

ACKNOWLEDGEMENTS

The authors wish to acknowledge Dr. Ronald Gronsky of the National Center for Electron Microscopy, Lawrence Berkeley Laboratory, for valuable discussions and continued encouragement. We would also like to thank Dr. Brian Sealy of the University of Surrey, England for Se^+ implantation. This work was supported by the Director, Office of Energy Research, Office of Basic Energy Sciences, Materials Science Division of the U.S. Department of Energy, under Contract No. DE AC03-76SF00098.

REFERENCES:

1. G.H. Narayanan and A. Kachare, Phys. Status Solid 26 657 (1974).

2. K. Gamo, T. Ineda, J.W. Mayer, F.H. Eisen and G.G. Rhodes, Rad. Eff. 33 85 (1977).

3. D.K. Sadana and G.R. Booker, Rad. Eff. 42 35 (1979).

4. S.S. Kular, B.J. Sealy, K.G. Stephens, D. Sadana and G.R. Booker, Solid State Electron 23 831 (1980).

5. J.S. Williams and M.W. Austin, App. Phys. Lett. 36 994 (1980).

6. M.G. Grimaldi, B.M. Paine, M-A Nicolet and D.K. Sadana, J. App. Phys. 53 1803 (1982).

7. R.S. Bhattacharya, A.K. Rai, P.P. Pronko, J. Narayan, S.C. Ling and S.R. Wilson, J. Phys. Chem. Solids 44 61 (1983).

8. S.S. Kular, B.J. Sealy and K.G. Stephens, Elec. Lett. 14 22 (1977).

9. D.K. Sadana, G.R. Booker, B.J. Sealy, K.C. Stephens and M.M. Badawi, Rad. Eff. 49 183 (1980).

10. T. Sands, D.K. Sadana, J. Washburn and R. Gronsky, (unpublished).

11. J. Washburn, C.S. Murty, D. Sadana, P. Byrne, R. Gronsky, N. Cheung and R. Kilaas, Nucl. Inst. & Meth. 209/210 345 (1983).

Figure Captions

Figure 1

a) Low magnification (110) cross section image of the unannealed sample. Note crystalline pockets at surface and heavily damaged amorphous-crystalline transition region between 2150 and 2500Å (depth scale indicated in nanometers).

b) Same magnification image of annealed sample. Note stacking fault bundles which initiate at 250Å and 2150Å and meet 1100Å below the surface (depth scale indicated in nanometers).

Figure 2

High magnification image of lower edge of transition region (at intersection of regions II and III of text). Note the amorphous pockets (which are partially buried in the TEM specimen). Several "channeled cascades" are visible below the interface. The level at 2500Å below the surface is indicated at left defocus - 900Å, upper arrow points to sample surface, depth scale indicated in nanometers).

Figure 3

Isolated extrinsic fault at a depth level of 2500Å (defocus - 1100Å). Note the dislocation adjacent to the lower end of the fault (arrow points to sample surface, depth scale indicated in nanometers).

Figure 4

Small bundles of stacking faults in annealed sample (defocus - 1100Å). These faults nucleated at 2250Å and grew until impingement with upper layer of faults at 1100Å (larger arrow points to sample surface, depth scale indicated in nanometers).

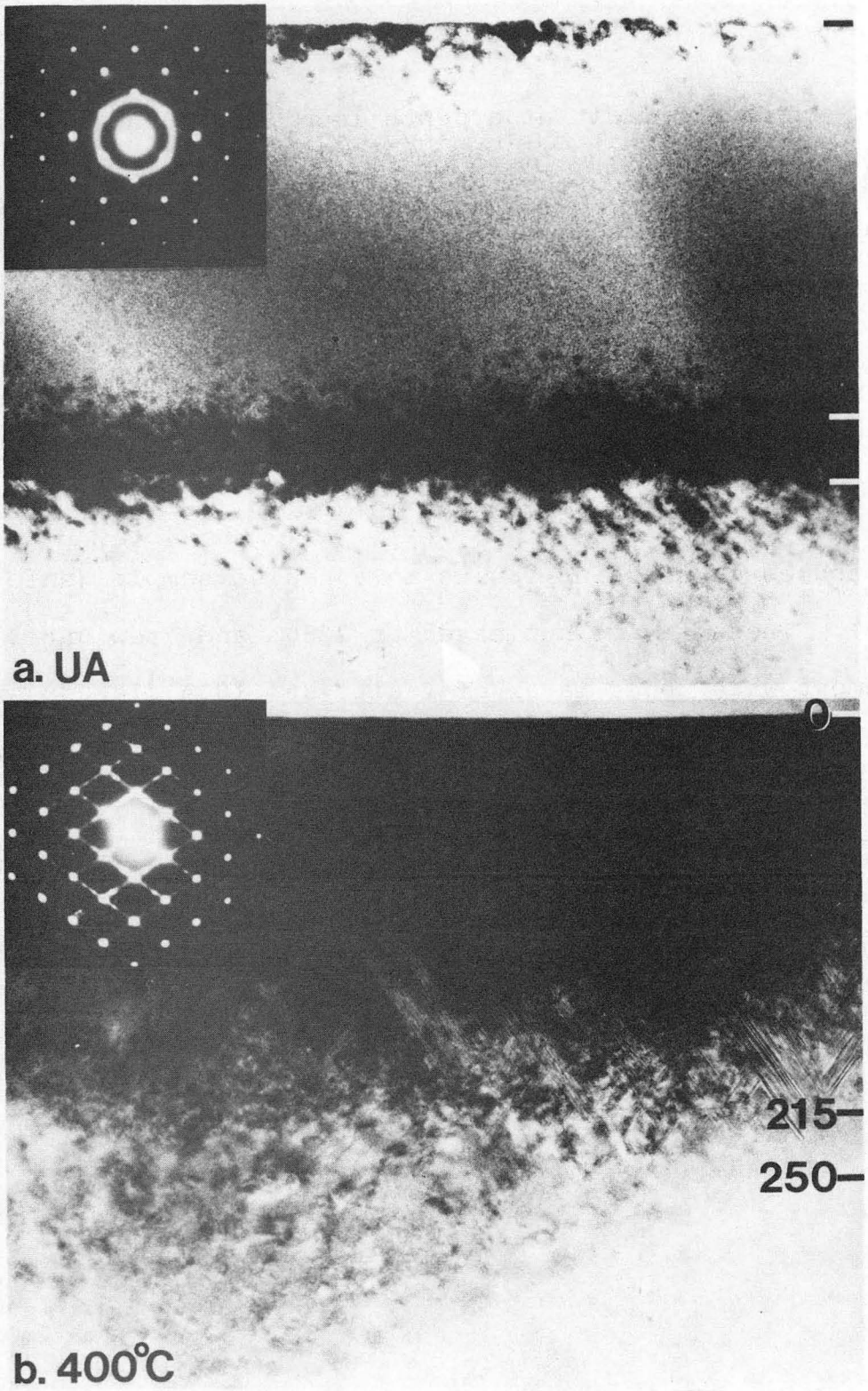

XBB 830-9404

Fig. 1

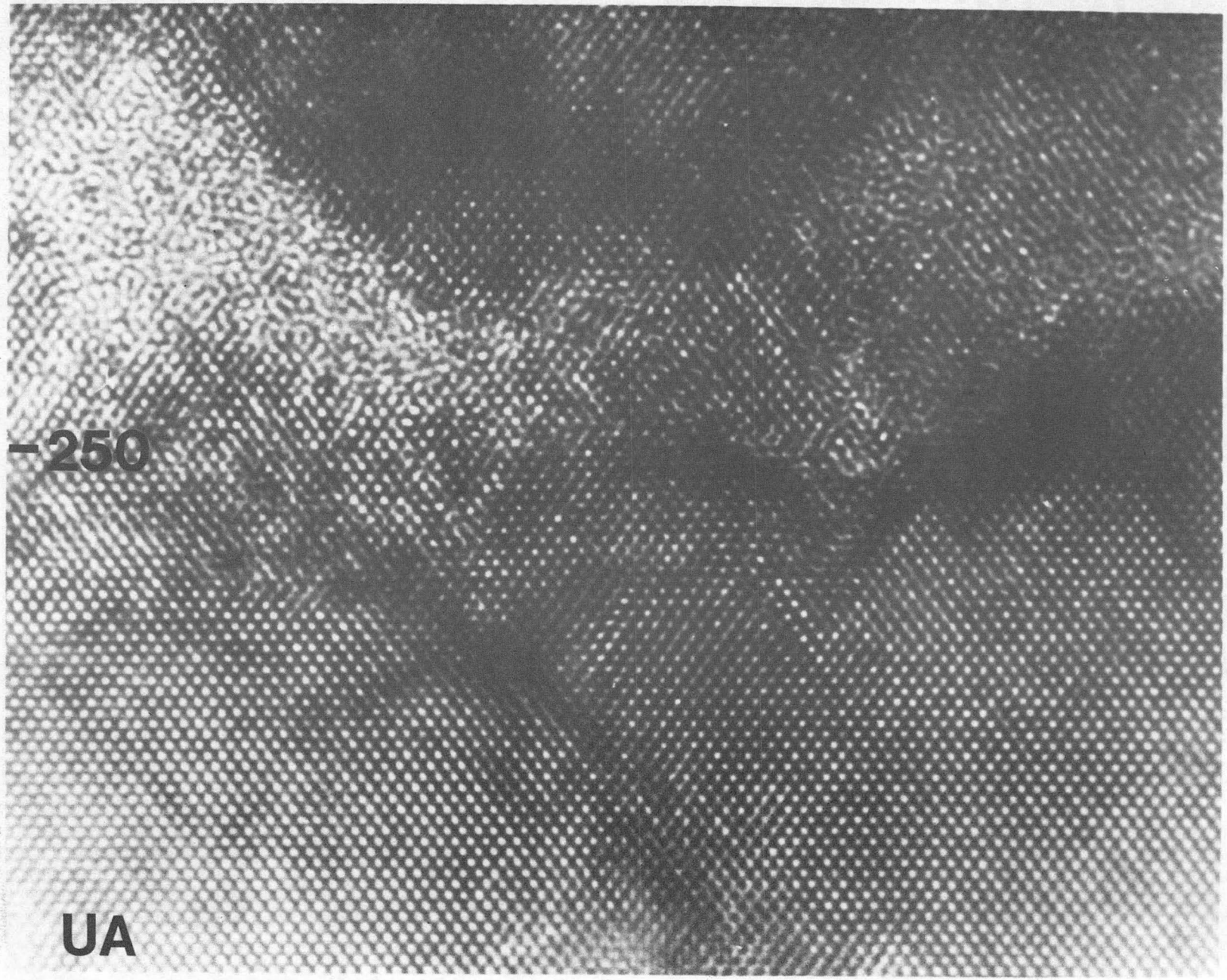

Fig. 2

XBB 830-9557

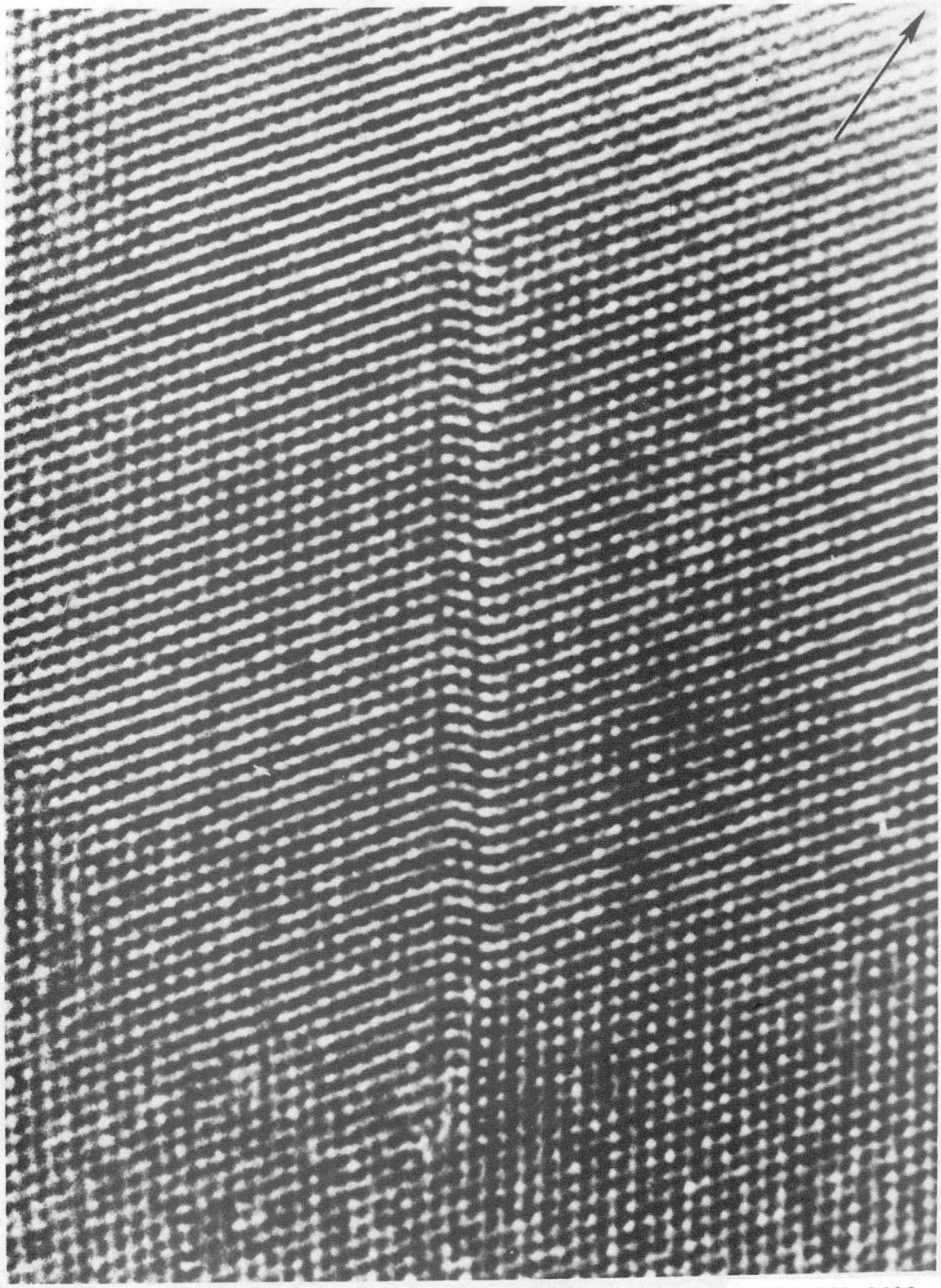

Fig. 3

XBB 830-9402

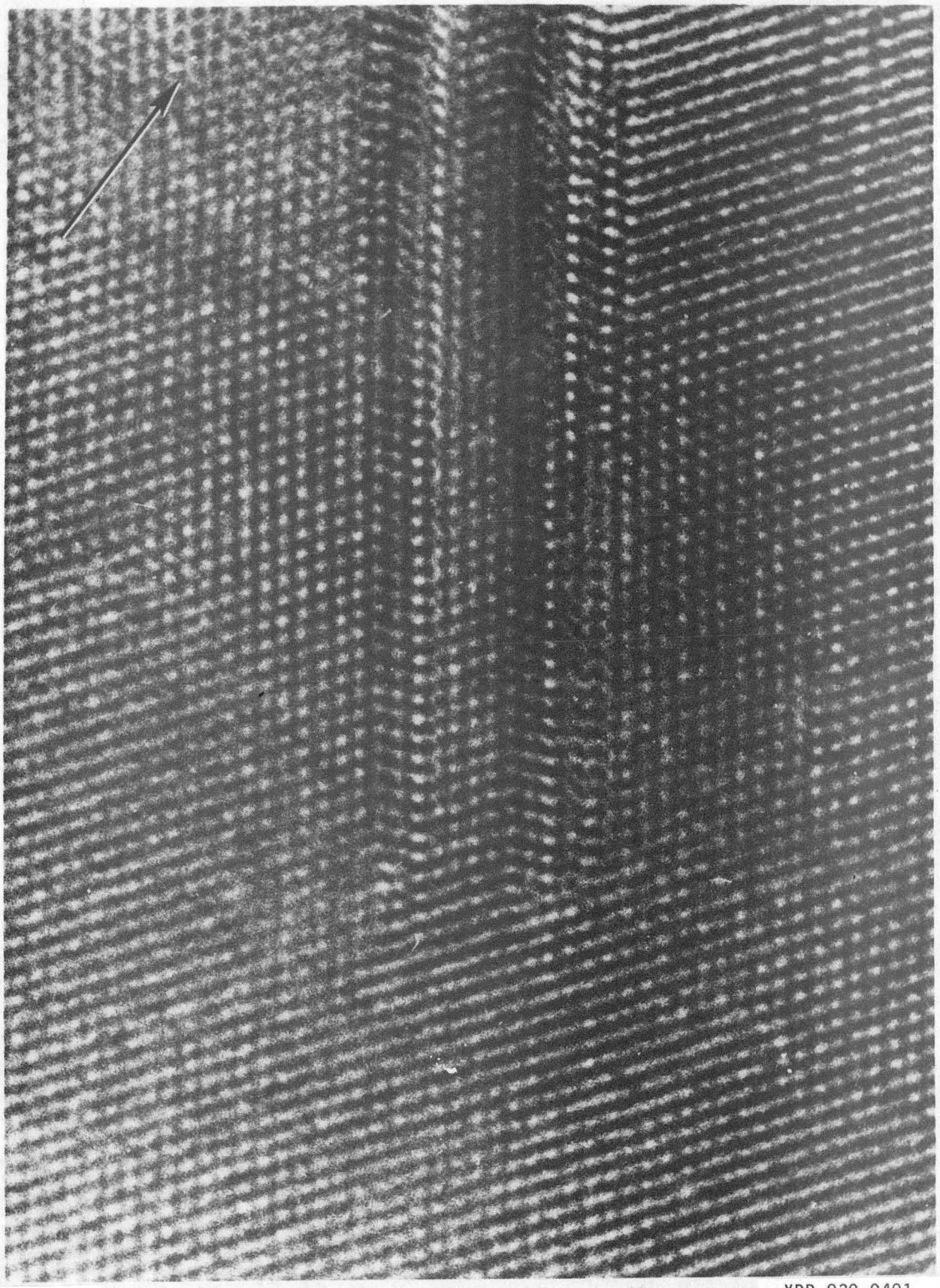

Fig. 4

XBB 830-9401

This report was done with support from the Department of Energy. Any conclusions or opinions expressed in this report represent solely those of the author(s) and not necessarily those of The Regents of the University of California, the Lawrence Berkeley Laboratory or the Department of Energy.

Reference to a company or product name does not imply approval or recommendation of the product by the University of California or the U.S. Department of Energy to the exclusion of others that may be suitable.

TECHNICAL INFORMATION DEPARTMENT
LAWRENCE BERKELEY LABORATORY
UNIVERSITY OF CALIFORNIA
BERKELEY, CALIFORNIA 94720